

Catalysis Science & Technology

Accepted Manuscript



This is an *Accepted Manuscript*, which has been through the Royal Society of Chemistry peer review process and has been accepted for publication.

Accepted Manuscripts are published online shortly after acceptance, before technical editing, formatting and proof reading. Using this free service, authors can make their results available to the community, in citable form, before we publish the edited article. We will replace this *Accepted Manuscript* with the edited and formatted *Advance Article* as soon as it is available.

You can find more information about *Accepted Manuscripts* in the [Information for Authors](#).

Please note that technical editing may introduce minor changes to the text and/or graphics, which may alter content. The journal's standard [Terms & Conditions](#) and the [Ethical guidelines](#) still apply. In no event shall the Royal Society of Chemistry be held responsible for any errors or omissions in this *Accepted Manuscript* or any consequences arising from the use of any information it contains.



www.rsc.org/catalysis



Catal. Sci. Technol.

COMMUNICATION

Electrocatalytic oxidation of water by a self-assembled oxovanadium(IV) complex modified gold electrode

Received 00th January 20xx,
Accepted 00th January 20xx

Koushik Barman^a and Sk Jasimuddin^{a*}

DOI: 10.1039/x0xx00000x

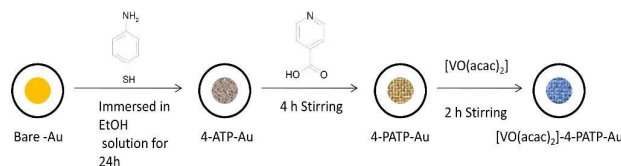
www.rsc.org/

Bis(acetylacetonato)oxovanadium(IV) was immobilized on the self-assembled 4-(pyridine-4'-amido)thiophenol (4-PATP) modified gold electrode. The modified electrode shows an excellent electrocatalytic activity towards water oxidation at neutral pH. The turn over frequency of the catalyst for water oxidation was 0.64 s⁻¹ at an overpotential ~ 284 mV (at J = 3.82 mA cm⁻²).

Water oxidation is a most crucial reaction in natural photosynthesis and is most schemes for artificial photosynthesis^{1,2}. Development of a robust, fast and inexpensive water oxidation catalyst still remains the most challenging task for artificial photosynthesis³. Water oxidation is the more kinetically demanding process and gives rise to a large part of the overpotential. Consequently, catalysts that allow electrochemical oxidation of water at low overpotential are of great interest^{4,5}. Although precious metals can show high catalytic activity for water oxidation at low overpotential, the high cost prohibits their widespread use^{6,7}. The creation of earth abundant molecular system that produced O₂ from water with high catalytic activity and stability thus remain a significant basic science challenge⁸. Both homogeneous and heterogeneous electrocatalyst have been developed for water oxidation. Among them, homogeneous molecular systems attract the most attention due to their straightforward synthesis, ease of characterisation, and tuneable properties. A large number of homogeneous water oxidation catalysts (WOCs) have been developed based on Mn^{9,10}, Fe^{11,12}, Cu¹³, Co^{14,15}, Ru^{16,17}, Ir^{18,19} complexes, and polyoxometalates^{20,21}. However, long term stability is an important issue. Most of them are transition-metal complexes with organic ligands, unstable toward oxidative deactivation. Heterogeneous catalysts for water oxidation were known long before their homogeneous analogues. They are thermodynamically stable, highly active and have long-life. Several heterogeneous catalysts have been developed for the electrochemical water oxidations,

some of them are Mn-oxide thin film on a polished GC electrode²², Mn₃O₄-Au nanocomposite on gold electrode²³, hydrated metal oxide modified electrode²⁴, Fe based film on ITO electrode²⁵, Co₃O₄ nanoparticles²⁶ and [Ni_{1-x}Fe_x(OH)₂](NO₃)_y(OH)_{x-y}·nH₂O nanosheet over flat HOPG surface²⁷, cobalt polyoxometalates (POM) carbon paste electrode²⁸, cobalt modified fluorine doped tin oxide electrode²⁹, Nickel oxy-hydroxide thin film³⁰, [Ru(bpy)₃][Ru₄POM] modified electrode⁴, iridium oxide-polymer composite electrode³¹, carbon grafted iridium complex³², IrO₂ colloied self-assembled on an ITO electrode⁶, mesoporous IrO_x nanoparticle film⁷ etc.

Terminal oxo complexes of transition metals have critical roles in various biological and chemical processes³³. For example, the catalytic oxidation of organic molecules³⁴, some oxidative enzymatic transformations³⁵, and the activation of dioxygen on metal surfaces³⁶ are all thought to involve oxo complexes. Moreover, they are believed to be key intermediates in the photocatalytic oxidation of water to give molecular oxygen^{37,38}. Natural photosystem(II) enzyme using a tetranuclear Mn-oxo complex as oxygen evolving center. Vandium complexes with high oxidation states are known to catalyze various oxidation reactions³⁹, such as oxidation of aldehydes⁴⁰ and thiols⁴¹, epoxidation⁴² and coupling⁴³. Additionally, vanadium plays an important role in enzyme reactions⁴⁴. These encourage us to prepare a simple self-assembled oxovanadium(IV) complex modified electrode for the electrocatalytic oxidation of water molecule. To our knowledge, this is the first report of catalytic water oxidation by vanadium complex modified electrode. Here we describe the preparation and surface characterisation of oxovanadium(IV) complex modified gold electrode and its application for the electrocatalytic oxidation of water at low overpotential in neutral pH.



Scheme 1 Electrode modification steps

^a Department of Chemistry, Assam University, Silchar, Assam-788011, India. E-mail: j.seikh@gmail.com, Phone No: 9435266930, Fax: 03842270806

* Footnotes relating to the title and/or authors should appear here.

Electronic Supplementary Information (ESI) available: [Experimental details, Figures, tables, additional results for electrochemical studies]. See DOI: 10.1039/x0xx00000x

COMMUNICATION

Catal. Sci. Technol.

The stepwise modification process (scheme 1) was monitored by cyclic voltammetry and electrochemical impedance spectroscopy using $[\text{Fe}(\text{CN})_6]^{3-/4-}$ as redox probe in 0.1 M PBS solution at pH 7.0.

(Figure S1). The fabrication of bis(acetylacetonato)oxovanadium(IV), $[\text{VO}(\text{acac})_2]$, over 4-(pyridine-4-yl-amido)thiophenol (4-PATP) modified Au electrode was confirmed by taking a comparable CV for 4-PATP-Au and $[\text{VO}(\text{acac})_2]$ -4-PATP-Au in 0.1 M PBS buffer at pH 7.0 (Figure S2). A quasireversible $\text{VO}^{\text{V}}/\text{VO}^{\text{IV}}$ redox couple ($E_{1/2} = 0.29$ V, $\Delta E = 70$ mV) supports the formation of $[\text{VO}(\text{acac})_2]$ modified 4-PATP-Au electrode. Figure S3 shows the cyclic voltammograms for different concentration (1.0 – 5.0 mM) of $[\text{VO}(\text{acac})_2]$ on the 4-PATP modified gold electrode. Both anodic and cathodic current increased linearly with increasing concentration of $[\text{VO}(\text{acac})_2]$ which confirms the strong electrostatic adsorption of $[\text{VO}(\text{acac})_2]$ at 4-PATP-Au electrode surface. The peak current varied linearly with the scan rate (30 – 90 mV/s) following the linear regression equation $J_{\text{pc}} (\mu\text{A}/\text{cm}^2) = 0.164 v (\text{mV}/\text{s}) + 4.131$ ($R^2 = 0.999$) which confirms the stability of the surface bound $[\text{VO}(\text{acac})_2]$ complex (Figure S4). The influence of pH of the electrolytic solution on the electrochemistry of $[\text{VO}(\text{acac})_2]$ -4-PATP-Au electrode was studied (Figure S5). The cathodic peak current reached the maximum value at pH 7.0 which indicate that at this pH strong complexation takes place.

The step wise modification and surface morphology of the bare gold electrode was characterised by FE-SEM. From the SEM images, it can be seen that the surface of the bare (Figure 1A) gold electrode was smooth and remain almost same (Figure 1B) after modification with 4-aminothiophenol (4-ATP) suggesting well ordered and densely packed layer formation. However, the surface morphology of 4-ATP-Au electrode was changed to a uniform wire-like structure (Figure 1C) after Schiff base condensation reaction between isonicotinic acid and 4-ATP-Au. Subsequent immobilization of $[\text{VO}(\text{acac})_2]$ over 4-PATP-Au electrode the surface was totally changed to a rough and porous (Figure 1D) morphology favourable for electrocatalytic oxidation. Elemental mapping images (Figure S6) confirms the immobilization of $[\text{VO}(\text{acac})_2]$ over 4-PATP modified gold electrode.

The self-assembled monolayer modified electrode, $[\text{VO}(\text{acac})_2]$ -4-PATP-Au was examined for the electrocatalytic water oxidation activity using cyclic voltammetry. The CV scans were carried out in the potential window -0.4 to 1.4 V versus Ag/AgCl with a scan rate of 0.1 V/s in 0.1 M PBS buffer at pH 7.0 (Figure 2). It was observed that the anodic peak potential for oxovanadium(IV) modified electrode shifted in the less positive potential with a large increase of current height compared to the bare or 4-PATP modified gold electrode. It supports the electrocatalytic activity of $[\text{VO}(\text{acac})_2]$ -4-PATP-Au modified electrode towards water oxidation. $[\text{VO}(\text{acac})_2]$ -4-PATP-Au electrode displayed an anodic response at + 0.89 V versus Ag/AgCl in 0.1 M PBS at pH 7.0, signifying water oxidation, $2\text{H}_2\text{O} \rightarrow \text{O}_2 + 4\text{H}^+ + 4\text{e}^-$. The oxidation peak current increased with the scan rate in the range of 0.02 to 0.2 V s^{-1} (Figure 3) following the linear regression equation $J_{\text{pa}} (\text{mA}/\text{cm}^2) = 0.0032 v (\text{mV}/\text{s}) + 0.1603$ ($R^2 = 0.999$). This indicates that the electro-oxidation reaction of water at oxovanadium complex modified electrode were the surface controlled process. Figure S7 shows the relationship between the peak potential (E_p) and the natural logarithm of scan

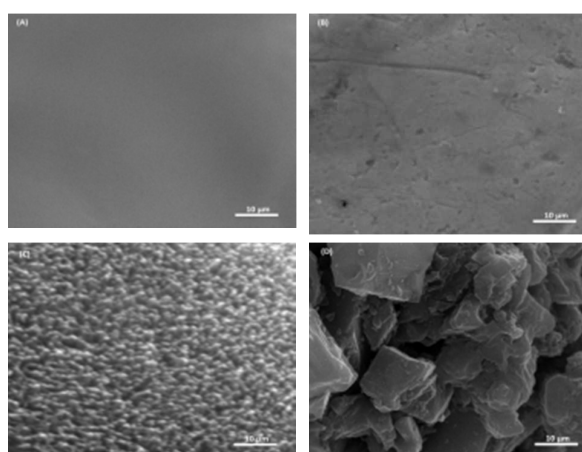


Fig. 1 SEM images of bare (A), 4-ATP modified (B), 4-PATP modified (C) and $[\text{VO}(\text{acac})_2]$ -4-PATP modified (D) gold electrode. (All scale bars are 10 μm)

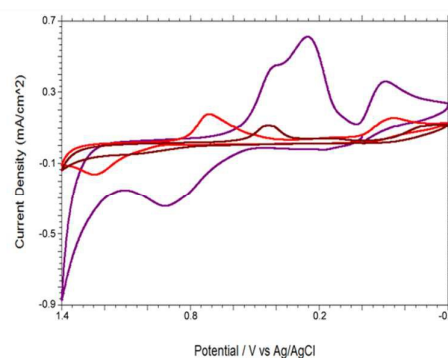


Fig. 2 Cyclic voltammograms obtained with bare (red curve), 4-PATP modified (brown curve) and $[\text{VO}(\text{acac})_2]$ -4-PATP modified (violet curve) gold electrodes in 0.1 M PBS at pH 7.0. Scan rate: 100 mV s^{-1} .

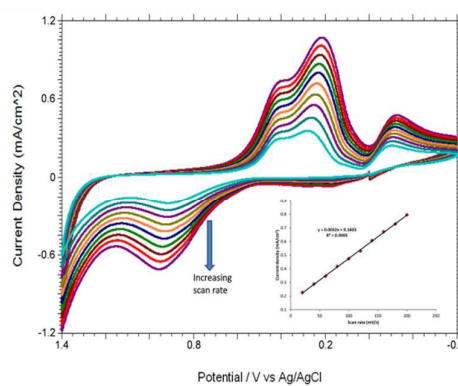


Fig. 3 Cyclic voltammograms from $[\text{VO}(\text{acac})_2]$ -4-PATP modified gold electrode at increasing scan rate 20 to 200 mV s^{-1} in 0.1 M PBS solution (pH 7.0), (Inset: Anodic peak current density versus scan rate plot).

rate ($\ln v$) for the water oxidation at modified electrode at pH 7.0. In the range from 0.02 – 0.2 V s^{-1} , the anodic peak potential (E_{pa}) changed linearly versus $\ln v$ with a linear regression equation of

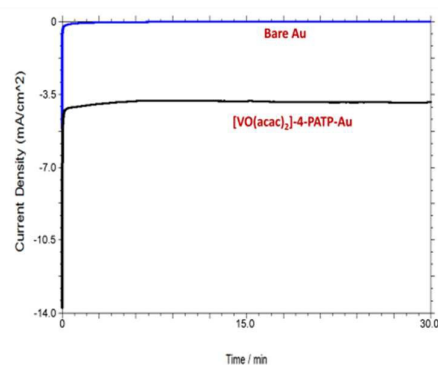


Fig. 4 Bulk electrolysis with (black curve) and without (blue curve) the $[\text{VO}(\text{acac})_2]$ catalyst over the 4-PATP-Au electrode in 0.1 M phosphate buffer (pH 7.0) at 0.89 V versus Ag/AgCl.

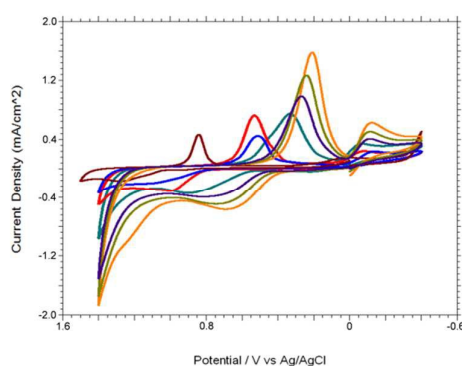


Fig. 5 Cyclic voltammograms derived from $[\text{VO}(\text{acac})_2]$ -4-PATP modified gold electrode at different pH (4.0, brown curve; 5.0, blue curve; 6.0, red curve; 7.0, green curve; 8.0, violet curve; 9.0, light green curve; 10, orange curve) of 0.1 M PBS solution. Scan rate: 100 mV s^{-1}

$E_{\text{pa}} = 0.803 + 0.028 \ln v$, $R^2 = 0.997$. Because of the irreversible electrode process of the water oxidation, the Laviron's equation⁴⁵: $E_{\text{pa}} = E^0 + RT/(1-\alpha)nF \{ \ln\{RTk_s/((1-\alpha)nF)\} + \ln v \}$ was used to estimate the number of electrons involved, where α is the anodic electron transfer coefficient, n is the number of electrons, k_s is the rate of electron transfer and R , T and F have their usual meaning. Here the slope of the linear plot, $RT/(1-\alpha)nF$ was 0.028, then n could be calculated to be 4.2 (theoretical value ought to be 4) since for a totally irreversible electron transfer, α was assumed as 0.5. This calculation indicated that anodic peak at + 0.89 V was due to 4 electrons water oxidation. The observed electrocatalytic water oxidation is quite exciting because of large current which indicate rapid rate and low overpotential. This oxidation occurred at an overpotential (η) of ~ 284 mV (vs NHE) (at $J = 3.8 \text{ mA/cm}^2$) which is within the typical range for many heterogeneous (200 - 400 mV) water oxidation catalyst^{46,47} and is quite better than many homogeneous (600-900 mV) water oxidation catalyst⁴⁸⁻⁵⁰. A Comparative overpotential is given in Table S1. The Tafel plot of η versus $\log J$ produce a slope of ~ 50 mV/decade (Figure S8) which indicates an outstanding activity of $[\text{VO}(\text{acac})_2]$ -4-PATP-Au electrode for electrolytic water oxidation.

In non-aqueous media no such oxidative or reductive peak was observed. Upon addition of water in CH_3CN solvent containing 0.1 M $[\text{Bu}_4\text{N}][\text{ClO}_4]$ (pH = 7.0) an oxidative peak appeared at ~ + 0.89 V. Initially the anodic peak current density increased with increasing the water concentration (up to 0.6 M) and thereafter the current density remain constant as expected for surface attached molecular species (Figure S9). Over several scan, the formation of gas bubbles was observed on the modified electrode surface (Figure S10). An irreversible cathodic peak around - 0.05 to - 0.1 V (depends upon pH) was observed only if the electrode was cycled to cathodic potential after scanning through the catalytic anodic wave under N_2 atmosphere (Figure S11a). Figure S11b shows the additional reduction current (~ 1.0 μA) when the potential was swept positively and then negatively in presence of O_2 . These results indicated that O_2 was evolved during water oxidation on the electrode surface. We have also tested the $[\text{VO}(\text{acac})_2]$ modified 4-PATP-Au electrode in acetate buffer solution instead of PBS solution (Figure S12) and in CH_3CN or $\text{CH}_3\text{CN} + \text{H}_2\text{O}$ mixed solvent containing 0.1 M $[\text{Bu}_4\text{N}][\text{ClO}_4]$ (pH = 7.0) (Figure S13) and confirmed that O_2 was generated solely due to water oxidation. The oxygen evolution was also investigated using controlled potential electrolysis at 0.89 V versus Ag/AgCl with a $[\text{VO}(\text{acac})_2]$ modified 4-PATP-Au electrode in 0.1 M PBS (pH 7.0) (Figure 4). The controlled potential electrolysis experiment shows that the current density rapidly declines to around 0.03 and 3.82 mA cm^{-2} for bare and oxovanadium modified gold electrode, respectively after ~ 20 seconds and thereafter the current remain stable over the entire course of electrolysis (30 minutes) in both cases (Figure S14). The result supports the high stability of $[\text{VO}(\text{acac})_2]$ -PATP modified gold electrode in the course of electrolysis. The oxygen formed in the solution was measured using a fluorescence probe (Figure S15). During the electrolysis of water the dissolved O_2 in the solution phase increased from ~ 30 μM to approximately 176 μM with a Faraday efficiency of around 98% for the O_2 evolution. On the basis of steady-state current measurement at an applied potential of 0.89 V versus Ag/AgCl at pH = 7.0, the apparent turnover frequency¹⁷ for water oxidation by the $[\text{VO}(\text{acac})_2]$ modified gold electrode was found 0.64 s^{-1} ($\text{TOF} = \text{catalytic current density/charge} = 3.82 \text{ mA cm}^{-2} / 5.97 \text{ mC cm}^{-2}$) at an overpotential of 284 mV (at $J = 3.82 \text{ mA cm}^{-2}$). Table 1 shows a comparison of the proposed electrochemical method and other modified electrodes reported for the oxidation of water. It can be seen that the overpotential and turnover frequency of the proposed method are comparable with the reported methods. The effect of pH on the electrocatalytic oxidation and reduction of water and oxygen, respectively at $[\text{VO}(\text{acac})_2]$ -4-PATP-Au electrode were investigated in the pH range 4.0 – 10.0. Figure 5 illustrates the cyclic voltammograms at varying pHs of the PBS for $[\text{VO}(\text{acac})_2]$ -4-PATP-Au electrode. Both the anodic and cathodic peak potentials were shifted towards more negative potential with increasing pH of the medium. The oxidation peak potential varies linearly with pH in basic media following the linear regression equation $E_{\text{pa}} (\text{V}) = -0.052 \text{ pH} + 1.222$ ($R^2 = 0.993$). Investigation of the influence of pH on the peak current density of water oxidation at the modified gold electrode revealed that the peak current also increases linearly with increasing solution pH. To explore the long term stability of the $[\text{VO}(\text{acac})_2]$ -4-PATP-Au electrode, cyclic voltammetry measurement were made in 0.1 M PBS solution with 15 days intervals (the modified electrode was stored by covering with a rubber cap at room temperature, when not in use) and the CV response were

COMMUNICATION

Catal. Sci. Technol.

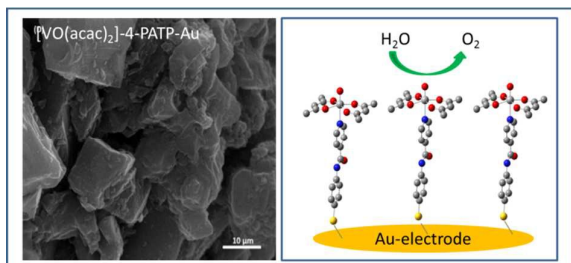
almost similar after 15 days and 30 days (RSD ~ 0.02 %) (Figure S16).

In summary, a new heterogeneous catalytic system [VO(acac)₂]-4-PATP-Au has made up for water oxidation. The oxovanadium complex modified gold electrode shows efficient water oxidation at reasonable low overpotential (~ 284 mV at J = 3.82 mA cm⁻²) with apparent TOF 0.64 s⁻¹ at neutral pH. This unique system is stable, reproducible, fast and inexpensive for water oxidation than many known systems. This outcome unlocks novel opportunities for energy conversion mechanism and fuel cell based research.

References

1. J. P. McEvoy, G. W. Brudvig, *Chem. Rev.*, 2006, **106**, 4455.
2. T. J. Meyer, *Nature*, 2008, **451**, 778.
3. H. Dau, C. Limberg, T. Reier, M. Risch, S. Roggan, P. Strasser, *Chem. Cat. Chem.*, 2010, **2**, 724.
4. S.-X. Guo, C.-Y. Lee, J. Zhang, A. M. Bond, Y. V. Geletii, C. L. Hill, *Inorg. Chem.*, 2014, **53**, 7561.
5. C. N. Cady, R. H. Crabtree, G. W. Brudvig, *Coord. Chem. Rev.*, 2008, **252**, 444.
6. M. Yagi, E. Tomita, S. Sakita, T. Kuwabara, K. Nagai, *J. Phys. Chem. B*, 2005, **109**, 21489.
7. T. Nakagawa, C. A. Beasley, R. W. Murray, *J. Phys. Chem. C*, 2009, **113**, 12958.
8. R. Eisenberg, H. B. Gray, *Inorg. Chem.*, 2008, **47**, 1697.
9. J. Limburg, J. S. Vrettos, H. Y. Chen, J. De Paula, G. W. Crabtree, R. H. Brudvig, *J. Am. Chem. Soc.*, 2001, **123**, 423.
10. J. Limburg, J. Vrettos, L. Liable-Sands, A. Rheingold, R. Crabtree, G. Brudvig, *Science*, 1999, **283**, 1524.
11. J. L. Fiollo, Z. Codola, I. Garcia-Bosch, L. Gomer, J. J. Pla, M. Costas, *Nat. Chem.*, 2011, **3**, 807.
12. W. C. Ellis, N. D. McDaniel, S. Bernhard, T. J. Collins, *J. Am. Chem. Soc.*, 2010, **132**, 10990.
13. S. M. Barnett, K. I. Goldberg, J. M. Mayer, *Nat. Chem.*, 2012, **4**, 498.
14. D. J. Wasylenko, C. Ganesamoorthy, J. B. Garcia, C. P. Berlinguette, *Chem Commun*, 2011, **47**, 4249.
15. S. G. Ferron, L. Vigara, J. S. Lopez, J. R. G. Mascaros, *Inorg. Chem.*, 2012, **51**, 11707.
16. K. Gong, F. Du, Z. Xia, M. Durstock, L. Dai, *Science*, 2009, **323**, 760.
17. L. Duan, A. Fischer, Y. Xu, L. Sun, *J. Am. Chem. Soc.*, 2009, **131**, 10397.
18. J. D. Blakemore, N. D. Schley, D. Balcells, J. F. Hull, G. W. Olack, C. D. Incarvito, O. Eisenstein, G. W. Brudvig, R. H. Crabtree, *J. Am. Chem. Soc.*, 2010, **132**, 16017.
19. N. D. McDaniel, F. J. Coughlin, L. L. Tinker, S. J. Bernhard, *J. Am. Chem. Soc.*, 2008, **130**, 210.
20. M. Murakami, D. Hong, T. Suenobu, S. Yamaguchi, T. Ogura, S. J. Fukuzumi, *J. Am. Chem. Soc.*, 2011, **133**, 11605.
21. Q. Yin, J. M. Tan, C. Besson, Y. V. Geletii, D. G. Musaev, E. Aleksey, A. E. Kuznetsov, Z. Luo, K. I. Hardcastle, C. L. Hill, *Science*, 2010, **328**, 342.
22. Y. Gorlin, T. F. Jaramillo, *J. Am. Chem. Soc.*, 2010, **132**, 13612.
23. H. Rahaman, K. Barman, S. Jasimuddin, S. K. Ghosh, *RSC Adv.* 2014, **4**, 41976.
24. R. L. Doyle, I. J. Godwin, M. P. Brandon, M. E. G. Lyons, *Phys. Chem. Chem. Phys.*, 2013, **15**, 13737.
25. Y. Wu, M. Chen, Y. Han, H. Luo, X. Su, M.-T. Zhang, X. Lin, J. Sun, L. Wang, L. Deng, W. Zhang, R. Cao, *Angew. Chem. Int. Ed.*, 2015, **54**, 4870.
26. J. D. Blakemore, H. B. Gray, J. R. Winkler, A. M. Müller, *ACS Catal.*, 2013, **3**, 2497.
27. B. M. Hunter, J. D. Blakemore, M. Deimund, H. B. Gray, J. R. Winkler, A. M. Müller, *J. Am. Chem. Soc.*, 2014, **136**, 13118.
28. J. S. Lopez, S. G. Ferron, L. Vigara, J. J. Carbo, J. M. Poblet, J. R. G. Mascaros, *Inorg. Chem.*, 2013, **52**, 4753.
29. C. A. Kent, J. J. Concepcion, C. J. Daves, D. A. Torelli, A. J. Rieth, A. S. Miller, P. G. Hoertz, T. J. Meyer, *J. Am. Chem. Soc.*, 2013, **135**, 8432.
30. M. E. G. Lyons, A. Cakara, P. O. Brien, I. Godwin, R. L. Doyle, *Int. J. Electrochem. Sci.*, 2012, **7**, 11768.
31. Y. Lattach, J. F. Rivera, T. Bamine, A. Deronzier, J. C. Moutet, *ACS Appl Mater Interfaces*, 2014, **15**, 12852.
32. K. E. Dekrafft, C. Wang, Z. Xie, X. S. Su, B. J. Hinds, W. Lin, *ACS Appl. Mater. Interfaces*, 2012, **4**, 608.
33. W. A. Nugent, J. M. Mayer, *Metal-Ligand Multiple Bonds* (Wiley, 1988).
34. B. Meunier [Ed.] *Biomimetic oxidations catalyzed by transition metal complexes* (Imperial College Press, 2000).
35. M. T. Green, J. H. Dawson, H. B. Gray, *Science*, 2004, **304**, 1653.
36. G. A. Somorjai, *Introduction to Surface Chemistry and Catalysis* (Wiley, 1994).
37. W. Ruettinger, G. C. Dismukes, *Chem. Rev.*, 1997, **97**, 1.
38. M. Yagi, M. Kaneko, *Chem. Rev.*, 2001, **101**, 21.
39. A. G. J. Ligtenbarg, R. Hage, B. L. Feringa, *Coord. Chem. Rev.*, 2003, **237**, 89.
40. D. Talukdar, K. Sharma, S. K. Bharadwaj, A. J. Thakur, *Synlett*, 2013, **24**, 963.
41. S. Raghavan, A. Rajender, S. C. Joseph, M. A. Rasheed, *Synth. Commun.* 2001, **31**, 1477.
42. T. Itoh, K. Jitsukawa, K. Kaneda, S. Teranishi, *J. Am. Chem. Soc.* 1979, **101**, 159.
43. C.-Y. Chu, D.-R. Hwang, S.-K. Wang, B.-J. Uang, *Tamkang J. Sci. Eng.* 2003, **6**, 65-72.
44. D. C. Crans, J. J. Smee, E. Gaidamauskas, L. Yang, *Chem. Rev.* 2004, **104**, 849-902.
45. E. Laviron, *J. Electroanal. Chem.* 1974, **52**, 355.
46. T. Nakgawa, N. S. Bjorge, R. W. Murray, *J. Am. Chem. Soc.*, 2009, **131**, 15578.
47. A. Minguzzi, F.-R. F. Fan, A. Vertova, S. Rondinini, A. J. Bard, *Chem. Sci.*, 2012, **3**, 217229.
48. W. C. Ellis, N. D. McDaniel, S. Bernhard, T. J. Collins, *J. Am. Chem. Soc.*, 2010, **132**, 10990.
49. H. W. Tseng, R. Zong, J. T. Muckerman, R. Thummel, *Inorg. Chem.*, 2008, **47**, 11763.
50. X. Sala, L. Romero, M. Rodriguez, L. Escriche, A. Llobet, *Angew. Chem. Int. Ed.* 2009, **48**, 2842-2852.

Table of contents



The oxo-vanadium(IV) complex modified gold electrode showed an efficient electrocatalytic activity towards water oxidation at neutral pH.